DOI: 10.15825/1995-1191-2025-3-117-124

ASSESSMENT OF BLOOD HEMOLYSIS DURING OPTIMIZATION OF THE ROTAFLOW CENTRIFUGAL PUMP IMPELLER

A.P. Kuleshov, N.V. Grudinin, A.S. Buchnev, V.A. Elenkin, D.N. Shilkin, V.K. Bogdanov Shumakov National Medical Research Center of Transplantology and Artificial Organs, Moscow, Russian Federation

This study focuses on the evaluation of a modernized impeller for the RotaFlow centrifugal pump (Maquet, Germany), carried out as part of efforts to design a domestic counterpart. The proposed impeller features a combination of primary elongated blades, responsible for generating the majority of pressure, and secondary shortened blades. The investigation examined pump performance under extracorporeal membrane oxygenation (ECMO) therapy conditions at a pressure of 350 mmHg and flow rate of 5 L/min. Computational analyses were conducted to evaluate fluid flow parameters associated with hemolysis risk. The optimized impeller demonstrated a significant increase in low tangential stress zones (<10 Pa), reduced exposure time, and a lower hemolysis index. Comparative mathematical modeling and bench testing with donor blood confirmed the improved hemodynamic performance of the redesigned impeller over the original configuration.

Keywords: hemolysis index, centrifugal pump, tangential stresses, impeller.

INTRODUCTION

In vitro evaluation of centrifugal heads for extracorporeal membrane oxygenation (ECMO) systems is often conducted under left ventricular bypass (LVB) conditions. In such studies, standard hemolysis testing is carried out using a validated method designed for LVB applications, typically at a pressure of 100 ± 5 mm Hg and a flow rate of 5 L/min on a dedicated test bench [1, 2].

In clinical practice, however, LV bypass pumps are frequently adapted for ECMO therapy. While these pumps are engineered to function within a specific flow and pressure range, they are often operated across a much broader spectrum of hemodynamic conditions, which results in a loss of efficiency.

A more effective strategy in this case is to develop centrifugal pump (CP) product lines, such as the Jarvik [3] or Excor [4] axial pump families. These lines incorporate pumps optimized for different flow and pressure ranges, enabling adaptation to various ECMO modes and oxygenators with different resistances.

However, it should be noted that implementing this strategy is very costly, and currently, CPs continue to serve as universal components for different ECMO operating modes. Under conditions requiring pressures of 300–400 mmHg to overcome oxygenator resistance and maintain flow rates of up to 5 L/min, pumps are often forced to operate outside their optimal range, which negatively impacts performance. This mismatch leads to a reduction in hydraulic efficiency, promoting the development of recirculation and turbulence zones,

particularly at lower flow rates. To compensate, the rotor speed must increase, which in turn exerts a harmful effect on blood elements. Moreover, it is well established that the thrombogenic potential of ECMO systems is linked to mechanical stress, which triggers activation of biochemical cascades [5]. This is mainly associated with blood–surface interactions in the wall layer and the mechanical impact of the impeller blades.

Hastings et al. [6] demonstrated that the CP, along with tubing and connectors, plays a key role in thrombus formation within the ECMO circuit. For this reason, CPs used in ECMO are routinely tested under elevated pressure conditions *in vitro*. For example, Li et al. [7] tested their device at 290 mmHg and 5 L/min, while patent studies of a Chinese CP model conducted at 350 mmHg and 5 L/min showed lower hemolysis rates compared to pumps tested under LVB test benches [8].

Methods of preliminary computer assessment of parameters [9, 10] are widely used for early evaluation of CPs. These approaches are particularly effective for assessing the risk of hemolysis, and are especially relevant when pumps must be tested under high-pressure operating conditions.

When analyzing mechanical effects, such parameters include shear stress (SN), denoted as τ , which, at a steady fluid velocity υ , changes linearly with distance (y) from the wall, regardless of the nature of movement [11] (1):

$$\tau = \mu \frac{dv}{dv}.$$
 (1)

The effect of shear stress (τ) is most pronounced near surfaces in direct contact with blood. On these surfaces,

Corresponding author: Arkady Kuleshov. Address: 1, Shchukinskaya str., Moscow, 123182, Russian Federation. Phone: (915) 292-47-98. E-mail: ilovemylene@yandex.ru

regions with different shear stress levels develop, directly influencing the formed elements of blood. Importantly, shear stress is closely linked to exposure time of blood to the mechanical components of the system: the longer the duration of contact, the higher the probability of hemolysis.

Erythrocytes can often withstand very high transient loads if the time spent passing through the pump is minimal. However, under relatively low shear stress conditions, prolonged stagnation within the pump can lead to hemoglobin release. This phenomenon is particularly relevant when pumps are operated outside their intended design range, especially at low flow rates.

A recent study by Gross-Hardt et al. [12] highlighted this problem. The authors examined ECMO pumps operating at flow rates of 0.5–1.5 L/min. Pumps originally designed for adults and children weighing >6 kg (with a flow capacity of 0.5–8.0 L/min) were applied in newborns weighing 3–6 kg, at flow rates as low as 0.3–0.5 L/min. The results demonstrated increased internal recirculation, elevated shear stress, and consequently higher levels of hemolysis.

As rotational speed increases, interactions between blood cells intensify, a phenomenon that, under turbulent flow conditions, is described by Reynolds stress [11] (2):

$$\tau = \varrho l^2 \left(\frac{d\upsilon}{dy}\right)^2. \tag{2}$$

This effect further contributes to hemolysis, underscoring the need to limit pump rotation speed in ECMO applications.

A reduction in the index of hemolysis (IH) under ECMO conditions has been reported by studies of the RotaFlow pump (Maquet, Germany) [11], which served as the basis for the present research and modernization. The proposed optimization method focuses on redesigning the impeller to enhance pump efficiency while lowering rotational speed. Such an approach is especially relevant when adapting pumps for ECMO. This can reduce hemolysis and improve pump performance under high loads.

The optimized design aims to reduce both specific energy consumption and exposure time, leading to a measurable improvement in the calculated IH. Validation of the concept was carried out under ECMO conditions using both computational modeling and *in vitro* bench testing.

MATERIALS AND METHODS

A computer model of the RotaFlow centrifugal pump (Maquet, Germany) was developed. At the initial stage, the pump components were scanned using a 3DMakerpro Seal 3D scanner (China), which enabled the creation of accurate sketches and three-dimensional (3D) models of all parts with a precision of 0.1 mm. The final assembly was rendered in the SolidWorks PhotoView 360 graphics

module, where the appropriate materials and textures were applied. The resulting model, shown in Fig. 1, replicates the mass and dimensional characteristics of the original pump.

The mass of the parts generated from SolidWorks materials corresponded closely to those of the original RotaFlow pump, with a total deviation of 0.5 ± 0.1 g. The redesigned impeller blade, compared with the original, is shown in Fig. 2. It consists of a rotor equipped with a primary elongated blade and a secondary shortened blade. The blade profile was defined with specific geometric parameters to reduce flow restriction while simultaneously increasing pressure generation during rotation. The shortened blade shares the same profile as the primary blade but has a length equal to one-third of the main blade.

The model was developed for numerical analysis of fluid flow. A 3D design was created for both the original impeller and the modified variant. The reference rotor, shown in Fig. 2, a, served as the base model, while the new impeller design, shown in Fig. 2, b, was evaluated relative to it. Among several design iterations, the selected impeller proved to be the most effective and optimal for the intended application.



Fig. 1. Reconstructed 3D model of the RotaFlow pump (Maquet, Germany)

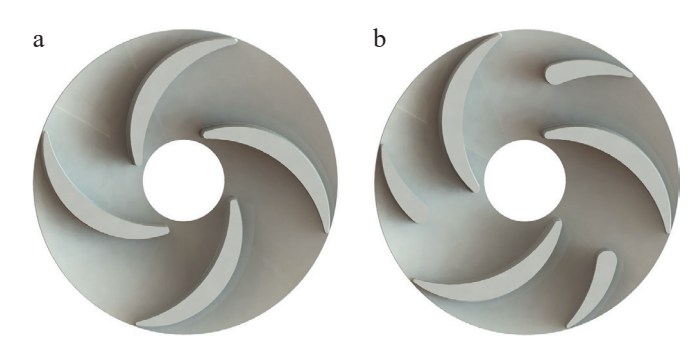


Fig. 2. Impeller blade profiles of the original (a) and modified (b) RotaFlow pump designs

Computational fluid dynamics (CFD) analysis

Numerical simulation of flow through the two pumps was performed using ANSYS Fluent 14.2. The flow distribution was obtained by solving the Navier–Stokes equations on an unstructured finite-volume grid. Boundary conditions were defined with zero pressure at the inlet and a fixed outlet pressure of 350 mm Hg. A flow rate of 5 L/min was achieved by adjusting the rotor speed.

Pump walls were assumed to be rigid with a surface roughness of 5 μ m, consistent with die-casting quality. Blood was modeled as an incompressible Newtonian fluid with a density of 1060 kg/m³ and a viscosity of 0.003763 Pa·s [13]. To solve the governing equations, the s-w turbulence model was applied, as it provides high efficiency and accuracy for near-wall flow conditions. A convergence criterion of 10^{-5} was used.

The computational mesh employed a minimum element size of $50 \, \mu m$ (tetrahedrons), which allowed calculations to be performed with minimal time and software costs.

Hemolysis index assessment

An important aspect of flow-induced blood damage is hemolysis, defined as the release of hemoglobin into plasma resulting from erythrocyte membrane damage. The two primary factors contributing to hemolysis are the shear stress generated by the pump and the duration of exposure of blood cells within the flow.

For engineering applications, the power-law equation proposed by Giersiepen et al. remains a widely used tool for estimating the amount of released hemoglobin (Δ Hb, expressed as a concentration relative to baseline hemoglobin, Hb). This model incorporates both exposure time and shear stress acting on red blood cells (3) [14]. Although it is well established that this equation tends to overestimate hemolysis and does not fully reproduce *in vivo* conditions, it continues to be applied successfully.

$$\frac{\Delta Hb}{Hb} = A \times t^{\alpha} \tau^{\beta}, \tag{3}$$

where τ is the shear stress acting on the blood, expressed in Pa, and t is the time of interaction of the blood within the shear field, expressed in seconds, and the relative increase in plasma hemoglobin is normalized in the range of 0–1. Different researchers have obtained empirical constants (A, α, β) by regression analysis of experimental hemolysis data. Two formulas obtained from different sources were used to solve the problems.

The first model applied was the well-known formulation by Thamsen and Affeld [15], which uses an Euler-based numerical approach to hemolysis prediction. The corresponding empirical coefficients are: $A = 3.62 \cdot 10^{-7}$, $\alpha = 0.785$, and $\beta = 2.416$. The second model was that of Heuser and Opitz [16], which defines a different set of coefficients: $A = 1.8 \cdot 10^{-6}$, $\alpha = 0.785$, $\beta = 1.991$. Both models were used to calculate the index of hemolysis (IH).

Following Thamsen et al. [15], the HI is defined as the integral of hemolysis productivity over the entire computational domain, normalized to the mass flow rate of intact blood entering the pump. Thus, we obtain a productivity term for hemolysis that includes shear stress and the cumulative damage carried over from the previous time step [15].

$$\frac{\Delta Hb}{Hb} = A \times t^{\alpha} \tau^{\beta}, \tag{4}$$

This equation reflects the nonlinear dependence of blood damage on exposure time (t) and served as the basis for determining the probable HI.

To evaluate the potential traumatic effect on blood flowing inside the pumps, shear stress was calculated on all surfaces in contact with blood. In addition, the exposure time of blood elements – defined as the residence time of blood within the pump from entry at the inlet to exit – was assessed. Different criteria have been proposed in the literature for the maximum permissible shear stress value for red blood cells.

Two key parameters influence blood trauma: shear stress and exposure time. An empirical curve developed by Leverett and Hellums [17] describes the relationship between these parameters. This curve is widely used to distinguish between two regimes of blood damage: one dominated by surface-induced hemolysis due to direct contact with pump walls, and the other by shear-induced hemolysis in the bulk flow.

Leverett and colleagues conducted experiments with concentric cylinder viscometers to investigate the combined effects of surface interaction, centrifugal forces, mixing, cell collisions, and viscous heating. The study confirmed that contact between red blood cells and solid surfaces significantly exacerbates blood trauma. Furthermore, they established a critical shear stress threshold of 150 Pa for concentric cylinder systems.

According to [16], the critical shear stress value is also 150 Pa, while other studies report higher thresholds of up to 250 Pa [18]. Importantly, zones of elevated shear stress may occupy only a small portion of the surface and be associated with very short erythrocyte exposure times. Therefore, to numerically determine the HI, the calculated average shear stress was used, determined along an average erythrocyte trajectory. By combining shear stress and exposure time, the models yielded an estimate of the expected average HI, expressed as the percentage increase in plasma free hemoglobin relative to the total hemoglobin content.

Creation of a bench sample

Based on preliminary computer simulations, 3D models of two centrifugal pump (CP) samples were created and exported to STL format. Using these files, physical parts of the mock-up were fabricated on a Formlabs 3B+ medical 3D printer (USA) by stereolithography (SLA).

This process employed a biocompatible, sterilizable surgical photopolymer, achieving a dimensional accuracy of 25 μm .

The fittings and blades were printed on a Stereotech Fiber 5D printer using the 5D Spiral Full method with PLA plastic. These elements were subsequently polished to achieve a smooth surface finish.

A 4-pole magnet, a 10 steel closing ring, and a custom-made support ball made of durable Al_2O_3 aluminum oxide (corundum, alundum) were integrated into the assembly unit. Prototype pumps with both the original and modified rotors, prepared for bench testing, are shown in Fig. 3. The CP housing is equipped with an outlet fitting with an internal diameter of $^3/_8$ inch. The impeller is driven by an external motor via a magnetic coupling.

Experimental tests were conducted on the developed CP, which was fitted with a single ball-bearing hybrid impeller and operated using a magnetic coupling. The drive system employed an Ex-Stream system motor (Biosoft-M, Russia), manufactured in accordance with the specifications described in this invention.

The Rotaflow pump prototypes weighed 61.3 ± 1.0 g with a priming volume of 32 ± 1 ml and were capable of delivering blood flow rates exceeding 10 L/min at normal rotation speeds between 1000 and 5000 rpm.

In vitro hemolysis testing

In vitro hemolysis was evaluated using a donor blood circulation circuit in accordance with the protocol recommended by the American Society for Testing and Materials (ASTM F1841-19). Each test was carried out on a bench setup containing 450 ml of donor blood (hematocrit: 38%, hemoglobin: 127 g/L). To assess the hemolytic performance of the two pumps, four hemolysis tests were conducted at a flow rate of 5.0 ± 0.2 L/min under two pressure conditions: 350 ± 5 mmHg and $100 \pm$



Fig. 3. Experimental photopolymer pump models with the original and modified rotor designs

5 mmHg. The blood reservoir was immersed in a water bath at 37 °C to maintain a constant blood temperature.

Volumetric flow rate was measured using a Transonic T410 ultrasonic flowmeter. Inlet and outlet pressures were monitored with BBraun sensors. Citrated blood had a hematocrit level of $40 \pm 2\%$.

The measurement procedure for free hemoglobin concentration followed the method described in [1]. Both the normalized index of hemolysis (NIH) and the modified index of hemolysis (MIH) were calculated as outlined in the same reference.

RESULTS

Distribution of shear stress on pump walls

To evaluate the distribution of shear stress, it was divided into three levels depending on the expected impact on blood cells: 1) shear stress <10 Pa – corresponds to physiological shear stress; 2) shear stress 10–100 Pa – may induce formation of high-molecular-weight compounds, degradation of von Willebrand factor (VWF), and platelet activation; 3) shear stress >100 Pa – represents non-physiological shear stress, associated with damage to blood components. An example of shear stress distribution within the pumps are illustrated in Figs. 4 and 5.

High shear stress was primarily observed at the trailing edges of the impeller blades and within the casing surface gaps. In the modified model, blood flow was more uniform, resulting in lower shear stress at the inlet. However, shear stress remained elevated along the blade edges. A significant difference was noted in the upper and lower gaps: the original model showed more extensive high-shear stress (red) zones at the gap inlet. These differences were evident under both standard LVB conditions (100 mmHg, 5 L/min) and ECMO conditions (350 mmHg, 5 L/min).

In LVB mode, most of the blood in both pumps was exposed to shear stress levels below 10 Pa. The main differences emerged in the distribution of zones up to 100 Pa and above. The modified impeller reduced loading in the gap regions and operated at a lower rotational speed, thereby reducing the pressure level above 100 Pa (Fig. 6, a). As expected, under ECMO conditions the percentage distribution shifted for both models compared to LVB mode. The overall area of high-shear stress zones increased significantly, although the relative difference between the models remained consistent (Fig. 6, b).

Average exposure time of blood in the modified and original designs was 0.22 s and 0.26 s, respectively, under operating conditions (350 mmHg, 5 L/min). At lower loading conditions (100 mmHg, 5 L/min), the exposure times were 0.24 s for the modified design and 0.31 s for the original design.

Under ECMO pressure conditions, the number of recirculation trajectories was lower than under LVB

conditions, resulting in a slight reduction of the average trajectory time despite identical flow rates. Since both pumps had nearly comparable priming volume, the modified model provided more effective flushing.

Analysis of mathematical and experimental hemolysis

The modified impeller design demonstrated a consistently lower potential IH compared to the original

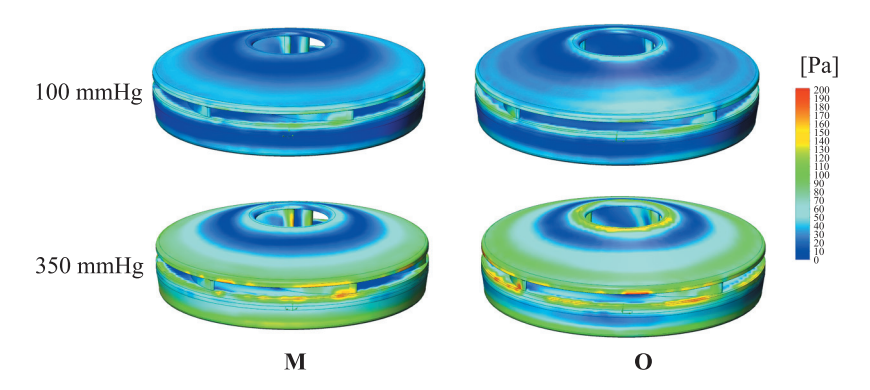


Fig. 4. Variation of tangential stress (TS) on the rotor surface for the modified (M) and original (O) impeller designs

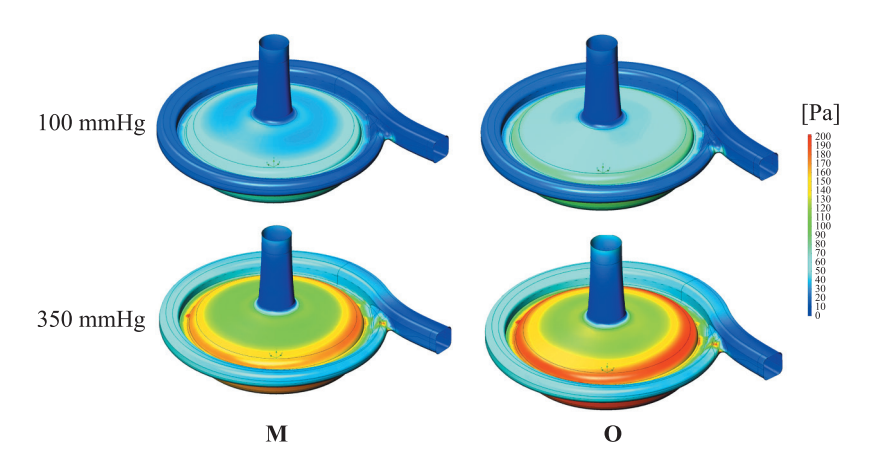


Fig. 5. Variation of tangential stress (TS) on the surface of the hull for the modified (M) and original (O) impeller designs

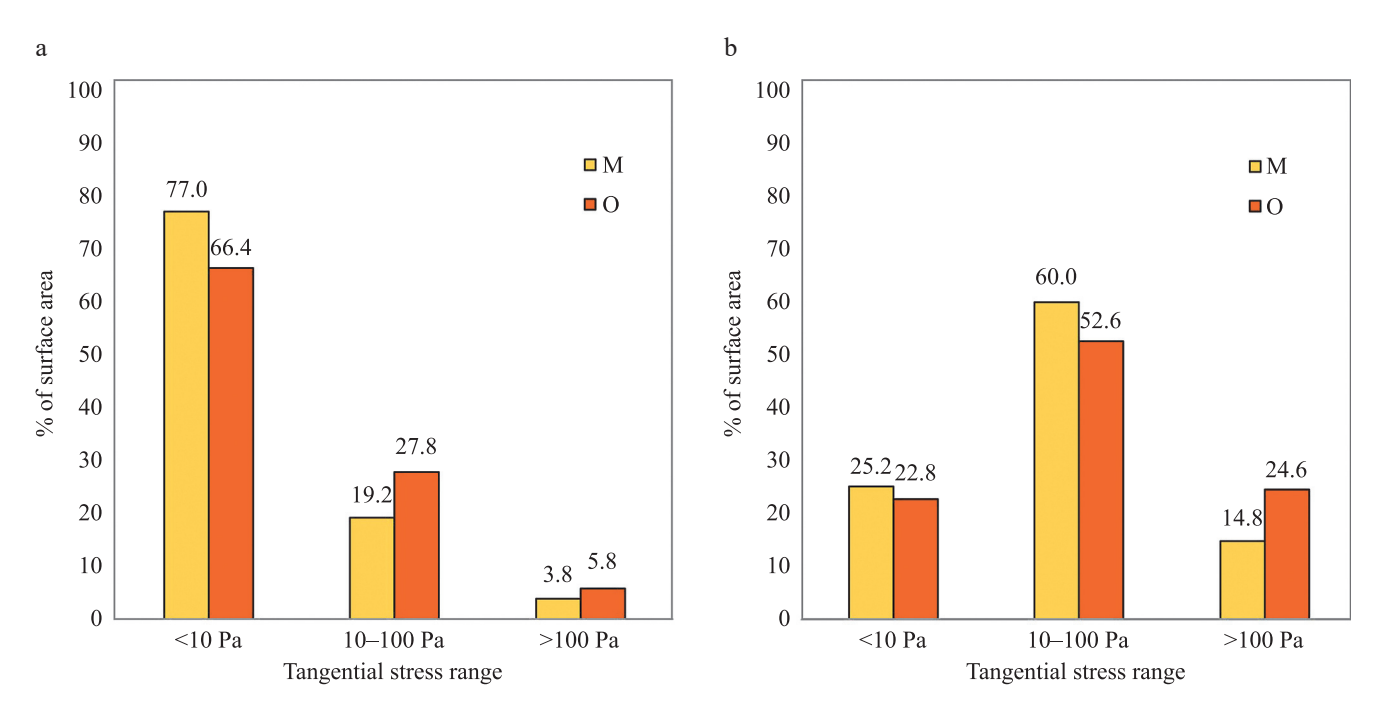


Fig. 6. Percentage distribution of tangential stress (TS) zones across three ranges in LVB mode (a) and ECMO mode (b)

Table Hemolysis parameters of models with original (O) and modified (M) rotors

Operating conditions	Pressure 100 mmHg, flow rate 5 L/min		Pressure 350 mmHg, flow rate 5 L/min	
	O	M	O	M
Impeller rotation speed, rpm	2155	2080	3560	3475
Maximum tangential stress (TS), Pa	250	238	504	462
Average TS, Pa	38	31	78	66
Average exposure time, s	0.31	0.24	0.26	0.22
Index of hemolysis (IH) growth model [15], ×10 ⁻⁴	9.46	4.47	46.84	27.45
IH growth model [16], ×10 ⁻⁴	10.00	5.47	36.53	23.00
IH model [18], based on coefficient from [15], $\times 10^{-3}$	3.41	2.20	20.15	14.02
IH model [18], based on coefficient from [16], $\times 10^{-3}$	3.48	2.45	15.05	11.10
NIH, g/100 L	0.00093	0.00084	0.00276	0.00254
MIH	0.1845	0.1677	0.5535	0.532

Rotaflow RC. At a hydraulic point of 100 mmHg and 5 L/min, the predicted IH was 1.21×10^{-4} for the modified model versus 1.77×10^{-4} for the original. Under ECMO conditions (350 mmHg, 5 L/min), the IH was 7.93×10^{-4} and 8.35×10^{-4} , respectively.

These predictions aligned with the experimentally measured NIH and MIH. At 100 mmHg and 5 L/min, the NIH was 0.00084~g/100~L for the modified model versus 0.00093~g/100~L for the original. Under ECMO loading conditions (350 mmHg, 5 L/min), the NIH values were 0.00254~g/100~L and 0.00276~g/100~L, respectively. The comparative parameters of both models are summarized in Table.

DISCUSSION

The dynamics of the IH generated by the centrifugal pump with the new rotor demonstrate excellent performance under clinically relevant ECMO support conditions. Both wall shear stresses and hemolysis characteristics were evaluated. Computational analyses showed that the average shear stress of the modified model was consistently lower than those of the original Rotaflow pump under identical operating conditions. This reduction is attributed to the unique impeller design, which achieves the required performance at a lower rotational speed.

Shear stress analysis further confirmed that the IH level of the modified model was lower compared to the Rotaflow pump. Since the numerically calculated IH depends on both exposure time and shear stress, and given that both pumps have nearly identical priming volumes, the shorter exposure time of the modified model indicates improved washability under the same operating conditions.

Therefore, the design of Model M, characterized by reduced shear stress, is expected to lower hemolysis. This assumption, based on IH assessment methods [18, 19], was validated by the experimentally measured NIH and MIH values for both pumps.

Calculations and tests on two CP prototypes demonstrated that hydrodynamic performance can be modestly improved without a complete redesign of the CP. This means that with this modification, the rotor speed can be reduced by 70–100 rpm, resulting in a 3–5% increase in hydraulic efficiency. This improvement is attributed to the enhanced flushing effect of the six blades, which more effectively flushes the flow from the central axial zone and thereby reduce exposure time. Shorter exposure time limits the duration of stress imposed on blood cells as they traverse the pump cavity.

The data obtained allow preliminary conclusions to be drawn regarding the quality of the modified design. It was observed that as impeller speed increases, the area of red blood cell exposure above 150 Pa also expands. Under ECMO conditions, these high-shear regions occupy up to 50% of the total flow area, inevitably increasing hemolysis. Nevertheless, shear stress distribution in the modified model proved more optimal compared to the original design.

The largest high-shear regions were located at the entrances to the gaps between the impeller and the casing (Fig. 5). In these zones, red blood cells reached maximum velocity and flow density and experienced strong turbulence from intense interactions with pump walls. The highest shear stress recorded in ECMO mode reached 504 Pa and 462 Pa, respectively.

The hemolysis values obtained in the experiments can be considered overestimated, as the tests were carried out on photopolymer prototypes whose relatively high surface roughness significantly influenced the results. However, the observed dynamics of hemolysis remain informative, and at this preliminary stage they support the relevance of the proposed modifications. The modified CP demonstrated good and predictable performance, and the results of laboratory experiments correlated well with the calculated data.

CONCLUSION

Computational fluid dynamics (CFD) analysis in computer-aided design systems is becoming a key tool for evaluating medical device designs. However, this tool has inherent limitations. Shear stress distributions calculated in centrifugal pumps are useful for preliminary assessment and serve as important indicators of potential hemolysis. However, conclusions drawn from CFD analysis must also incorporate the exposure time of blood cells at the given shear stress level.

When designing ECMO pumps, two critical factors must be considered: minimizing blood trauma and maintaining a low priming volume, which is especially important in pediatric applications. The flow path must therefore include smooth transitions and a highly efficient impeller capable of operating at minimal rotational speeds and relatively low flow rates, as required for centrifugal systems. Achieving high efficiency under these conditions is challenging, and operating pumps across their entire pressure—flow range is not rational. Significant deviations from the optimal operating point inevitably reduce hydraulic efficiency and alter flow dynamics.

The proposed invention represents a new technical solution within the class of implantable blood pumps. It is industrially applicable, as the pump components have been specifically designed for manufacturability, including molding processes and simplified assembly and bonding methods.

It can be concluded that the transition to a rotor with three long and three short blades offers clear advantages. Nevertheless, the development of a full product line of pumps, capable of covering the necessary range of flows and pressures for different patients remains a priority.

The authors declare no conflict of interest.

REFERENCES

- 1. *Itkin GP, Bychnev AS, Kuleshov AP et al.* Haemodynamic evaluation of the new pulsatile-flow generation method *in vitro. The Inter-national Journal of Artificial Organs.* 2020; 43 (6): 157–164.
- Roberts N, Chandrasekaran U, Das S et al. Hemolysis associated with Impella heart pump positioning: In vitro hemolysis testing and computational fluid dynamics modeling. Int J Artif Organs. 2020. Mar 4: 391398820909843. doi: 10.1177/0391398820909843.
- 3. *Kilic A, Nolan TD, Li T et al.* Early *in vivo* experience with the pediatric Jarvik 2000 heart. *ASAIO J.* 2007; 53 (3): 374–378. doi: 10.1097/MAT.0b013e318038fc1f.
- 4. Schmid C, Tjan T, Etz C et al. The excor device revival of an old system with excellent results. Thorac Cardiovasc Surg. 2006; 54 (6): 393–399. doi: 10.1055/s-2006-924268.

- Liu GM, Jin DH, Jiang XH et al. Numerical and In Vitro Experimental Investigation of the Hemolytic Performance at the Off-Design Point of an Axial Ventricular Assist Pump. ASAIO J. 2016; 62 (6): 657–665. doi: 10.1097/MAT.00000000000000429.
- Hastings SM, Ku DN, Wagoner S et al. Sources of circuit thrombosis in pediatric extracorporeal membrane oxygenation. ASAIO J. 2017; 63: 86–92.
- 7. *Li P, Mei X, Ge W et al.* A comprehensive comparison of the *in vitro* hemocompatibility of extracorporeal centrifugal blood pumps. *Front Physiol.* 2023. May 9; 14: 1136545. doi: 10.3389/fphys.2023.1136545.
- Zhongjun WU. US20240198080A1/ Improved centrifugal blood pump. 2024.
- Kuleshov AP, Itkin GP, Buchnev AS, Drobyshev AA. Mathematical evaluation of hemolysis in a channel centrifugal blood pump. Russian Journal of Transplantology and Artificial Organs. 2020; 22 (3): 79–85. https://doi.org/10.15825/1995-1191-2020-3-79-85.
- Sarfare S, Ali MS, Palazzolo A, Rodefeld M, Conover T, Figliola R et al. Computational Fluid Dynamics Turbulence Model and Experimental Study for a Fontan Cavopulmonary Assist Device. J Biomech Eng. 2023 Nov 1; 145 (11): 111008. doi: 10.1115/1.4063088.
- 11. *Lomakin AA*. Tsentrobezhnye i osevye nasosy. 2-e izd. pererab. i dop. M.–L.: Mashinostroenie, 1966; 364.
- 12. *Gross-Hardt S, Hesselmann F, Arens J et al.* Low-flow assessment of current ECMO/ECCO2R rotary blood pumps and the potential effect on hemocompatibility. *CritCare*. 2019; 23: 348.
- Fiusco F, Broman LM, Prahl Wittberg L. Blood Pumps for Extracorporeal Membrane Oxygenation: Platelet Activation During Different Operating Conditions. ASAIO J. 2022; 68 (1): 79–86. doi: 10.1097/ MAT.00000000000001493.
- 14. Giersiepen M, Wurzinger LJ, Opitz R, Reul H. Estimation of shear-related blood damage in heart valve prostheses in vitro comparison of 25 aortic valves. Int J Artif Organs. 1990; 13: 300–306.
- 15. *Thamsen B, Blümel B, Schaller J et al.* Numerical analysis of blood damage potential of the HeartMate II and HeartWare HVAD rotary blood pumps. *Artificial Organs*. 2015; 39 (8): 651–659.
- 16. *Heuser G, Opitz R*. A Couette viscometer for short time shearing of blood. *Biorheology*. 1980; 17: 17–24.
- 17. Leverett L et al. Red Blood Cell Damage by Shear Stress. *Biophysical Journal*. 1972; 3 (12): 257–273.
- Fang P, Du J, Yu S. Effect of the Center Post Establishment and Its Design Variations on the Performance of a Centrifugal Rotary Blood Pump. Cardiovasc Eng Technol. 2020; 11 (4): 337–349. doi: 10.1007/s13239-020-00464-0.

The article was submitted to the journal on 23.06.2025